

Two-state Brownian motor driven by synchronously fluctuating unbiased forcesV. M. Rozenbaum,^{1,2,3,*} Yu. A. Makhnovskii,^{1,4} S.-Y. Sheu,⁵ D.-Y. Yang,^{1,†} and S. H. Lin^{1,2}¹*Institute of Atomic and Molecular Sciences, Academia Sinica, Taipei 106, Taiwan*²*Department of Applied Chemistry, National Chiao Tung University, 1001 Ta Hsuen Road, Hsinchu, Taiwan*³*Chuiko Institute of Surface Chemistry, National Academy of Sciences of Ukraine, Generala Naumova street 17, 03164 Kiev, Ukraine*⁴*Topchiev Institute of Petrochemical Synthesis, Russian Academy of Sciences, Leninsky Prospect 29, 119991 Moscow, Russia*⁵*Department of Life Sciences and Institute of Genome Sciences, Institute of Biomedical Informatics,**National Yang-Ming University, Taipei 112, Taiwan*

(Received 1 May 2011; published 4 August 2011)

As a model of the Brownian motor, we consider a particle moving unidirectionally under the action of two synchronously fluctuating unbiased forces, transverse and longitudinal with respect to the particle track. The former force induces track-normal transitions of the particle between the attached and detached states (with and without a periodic potential, respectively), whereas the latter drives track-parallel motion in either state. Analytical expressions of the current and efficiency are derived for different regimes, with due account of the delayed response of the system to force fluctuations. For a sawtooth potential in the attached state, we reveal several motion regimes affording the maximum current or the maximum efficiency. A special emphasis is placed on the possibility of current reversal. As shown, the interplay between two phase-shifted harmonically varied forces as well as inherent and externally induced asymmetry can lead to the emergence of multiple current reversals, thus enabling the flexible controllability of the motion direction.

DOI: [10.1103/PhysRevE.84.021104](https://doi.org/10.1103/PhysRevE.84.021104)

PACS number(s): 05.40.-a, 05.60.Cd, 82.20.-w, 87.16.Nn

I. INTRODUCTION

In systems possessing vectorial symmetry, a Brownian particle subjected to external unbiased perturbations, deterministic or stochastic, can exhibit a net drift even in the absence of any long-range gradient [1–3]. The models for this phenomenon generically called *ratchets* or *Brownian motors* [4] have received much attention in recent years and have been discussed in manifold contexts [1–12]. The Brownian motor concept is primarily aimed at gaining insight into the operation principles of molecular motor proteins [13] and ion pumps [14]. Another motivation comes from artificial molecular and nanoscale machinery design [10–12,15]. Two main paradigms are recognized in this concept: *flashing* ratchets [16–18] in which transported particles are exposed to a time-fluctuating binding potential along their periodic track, and *rocking* ratchets [19–21] in which the particles move in an asymmetric periodic potential under the action of a spatially uniform time-dependent zero-mean force. The properties of the two ratchet types essentially differ in the adiabatic limit and are characterized by the various mechanisms of current reversal [22,23].

In inherently symmetric systems, directed motion can emerge through the dynamical breaking of left-right symmetry. There are a few essentially different ways, based on the nonlinearity of the substrate, to bring about spatial asymmetry by external perturbations. The most commonly used way is to apply a temporally asymmetric, though zero-mean, driving force to a particle moving in a symmetric periodic potential; a so-called asymmetrically tilting ratchet is thus formed [24–27]. A particular realization of this approach known as harmonic mixing is the generation of a dc output by two

superimposed sinusoidal ac input signals at commensurate frequencies [28–31]. Another nonlinear mechanism leading to motion rectification is gating, which originates from the combined action of a modulated spatially symmetric potential and an external time-symmetric ac force [32,33]. To provide the gating effect, the perturbations must be synchronized so that potential barriers lower in the first half-period at the same time as the particle is pushed, say to the right, while the barriers rise in the second half-period when the driving force acts oppositely. The above-outlined nonlinear mechanisms illustrate a potentially general approach to produce directed motion in response to unbiased nonequilibrium perturbations; this strategy suggests the combined use of two input signals in which the rectification of one of them is induced or enhanced by the other (nonlinear signal mixing [32,33]). Such an approach involving a subtle interplay of nonlinearity, asymmetry, signal parameters, and thermal noise offers great promise to achieve controllable motion on the nanoscale [9,12] and is definitely interesting for further analysis.

In the present work, we exploit the idea of nonlinear signal mixing invoking a simple two-state model in which a Brownian particle moving along a track stays in either an attached or a detached state, with and without a periodic potential, respectively. The track-parallel motion of the particle in either state is driven by a longitudinal fluctuating unbiased force. Track-normal transitions between the states occur under the action of another fluctuating force, a transverse one. The combination of the two synchronized force signals gives rise to directed motion of the particle. We focus on various regimes of the directed motion, depending on the model parameters. The motivation for this research comes primarily from the fact that more effective rectification of a signal by a ratchet device can be achieved by adding another signal of controlled frequency, amplitude, and phase. Additionally, we undertook the present work to clarify the effect caused on the motor operation by the system delayed response to the forcing.

*vik-roz@mail.ru, vrozen@pub.iams.sinica.edu.tw

†dyang@pub.iams.sinica.edu.tw

At first glance, the model considered here resembles rocked-pulsated ratchet devices previously reported in Refs. [32–34]. However, our model differs from that in Ref. [34] both in formulation (the latter involves the fast flashing of an asymmetric potential not synchronized with an unbiased force oscillation) and the resulting effect (the latter behaves as a mere superposition of the flashing and rocking ratchets, thus yielding no directed motion in a symmetric potential). Nor do the rocked-pulsated schemes [32,33], though working in a symmetric potential (via the gating mechanism), cover our model: we assume that the transverse force effect is irreducible to a certain time dependence of the potential energy amplitude because the force fluctuations and the energy amplitude are related dynamically [22]. A sketch of our approach was discussed in terms of the so-called low-energy approximation, compared to the concepts of flashing and rocking ratchets [22], and implemented as a near-surface Brownian motor [35].

In contrast to the previous studies, the present two-state consideration includes the effect of a delayed system response to external force signals. The emphasis is made on the possibility of current reversal resulting from the interplay of two phase-shifted harmonically varied applied forces and the competition between the inherent and externally induced asymmetry of the system. As further shown, the model operates in several motion regimes affording the maximum current or the maximum efficiency.

II. THE MODEL

Consider a Brownian particle moving in a two-dimensional potential $V(x, z)$ under the action of a two-component time-periodic force $\mathbf{F}(t) = (F_x(t), F_z(t))$: $\mathbf{F}(t + \tau) = \mathbf{F}(t)$, where τ is a period. As a function of z , the potential is assumed to have two minima at $z_a = -H/2$ and $z_d = H/2$ separated by a high barrier V_z at $z = 0$. This allows one to consider the particle motion as driven diffusion along two x -parallel tracks at z_a and z_d combined with random hopping from one track to the other (see Fig. 1). The two tracks referring to the attached and detached states are characterized by different potential profiles: $V(x, z_a) = V_a(x)$ and $V(x, z_d) = V_d(x) = 0$, where $V_a(x + L) = V_a(x)$ is a periodic function. Thus the particle motion is hindered in the former state and is free in the latter. The applied forces, $F_x(t)$ and $F_z(t)$, drive the system out of equilibrium. If they also break the system symmetry [due to a specific synchronization of the forces or a temporal asymmetry of $F_x(t)$] or the symmetry is initially broken, the directed motion occurs. Otherwise, enhanced diffusion is observed [36,37].

With this setup, it is reasonable to treat the x motion of the particle in terms of the continuous Fokker-Planck-Smoluchowski description extended with sink and source terms and the z motion in terms of the discrete kinetic approach. Then the joint probability density $p_q(x, t)$ for the particle to be in the attached or detached state ($q = a, d$) at position x at time t satisfies two Smoluchowski equations with the sink and source term $r(x, t)$ accounting for the random interstate transitions with the position-dependent rate constants $\gamma_{ad}(x, t)$ and $\gamma_{da}(x, t)$ (see, e.g., Refs. [1,3,8] where a similar description

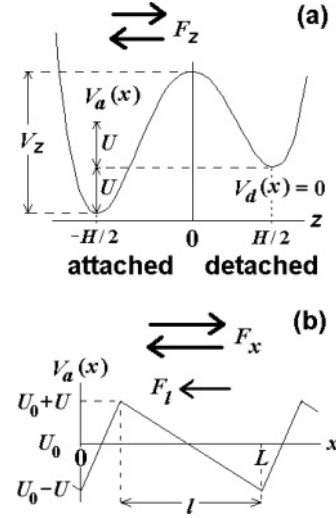


FIG. 1. The scheme of the model represented by the x cross section (a) and the z cross section at $z = H/2$ (b) (see the text for more details). Here U and U_0 are the amplitude and the average value of the potential $V_a(x)$ relative to the energy of the detached state $V_d(x) = 0$. In panel (a), the value of U_0 is chosen equal to zero.

has been used):

$$\begin{aligned} \frac{\partial}{\partial t} p_q(x, t) &= -\frac{\partial}{\partial x} J_q(x, t) \mp r(x, t), \\ r(x, t) &\equiv \gamma_{ad}(x, t) p_a(x, t) - \gamma_{da}(x, t) p_d(x, t), \\ J_q(x, t) &= -D e^{-\beta V_q[x; F_x(t)]} \frac{\partial}{\partial x} [e^{\beta V_q[x; F_x(t)]} p_q(x, t)], \\ \gamma_{qq'}(x, t) &= \gamma e^{\beta V_q(x) - \beta F_z(t) z_q}, \quad \gamma = \gamma_0 e^{-\beta V_z}, \\ V_q[x; F_x(t)] &\equiv V_q(x) - F_x(t)x, \quad q = a, d, \end{aligned} \quad (1)$$

where $\beta \equiv (k_B T)^{-1}$ ($k_B T$ is the thermal energy), $D = k_B T / \zeta$ is the diffusion coefficient (ζ is the friction coefficient) referring to potential-free unrestricted Brownian motion, and the characteristic frequency γ_0 is determined by the curvatures of minima and maxima of the potential in the x cross section. The validity of the description used is provided by the inequalities: $\beta V_z \gg 1$ and $\tau^{-1} \ll \gamma_0$. Both probability densities and probability currents must satisfy periodic boundary conditions at $x = 0$ and L . In view of Eq. (1), this implies that the probability $\rho_q(t)$ to find the particle in state q defined as

$$\rho_q(t) \equiv \int_0^L p_q(x, t) dx \quad (2)$$

satisfies the following equation:

$$\frac{d}{dt} \rho_q(t) = \mp \int_0^L r(x, t) dx. \quad (3)$$

We are concerned with sufficiently long times to assume that the path traversed by the particle extends far beyond the period L and the quantities of interest become periodic functions of time. Of primary significance is the average velocity of the particle, \mathfrak{U} , which is expressible in terms

of the total probability current $J(x,t) = J_a(x,t) + J_d(x,t)$ as follows:

$$\mathcal{A} = \int_0^L dx \langle J(x,t) \rangle. \quad (4)$$

Hereinafter, the angle brackets denote averaging over the period. Another relevant quantity is the energetic efficiency with which the motor converts external fluctuations into useful work [8], e.g., advances against a constant load force F_l [so that the resultant longitudinal force acting on the particle is $F_x(t) - F_l$]. The energetic efficiency η is defined as the ratio of the power output P_{out} to the power input P_{in} . Note that P_{in} includes two contributions $P_{\text{in}}^{(x)}$ and $P_{\text{in}}^{(z)}$ reflecting the power consumption for maintaining nonequilibrium distributions along the x and z directions, required for the system to operate as a Brownian motor. These main characteristics of the energy conversion process can be specified by the following relations:

$$\begin{aligned} P_{\text{out}} &= F_l \mathcal{A}, \quad P_{\text{in}} = P_{\text{in}}^{(x)} + P_{\text{in}}^{(z)}, \quad \eta = P_{\text{out}}/P_{\text{in}}, \\ P_{\text{in}}^{(x)} &= \int_0^L dx \langle F_x(t) J(x,t) \rangle, \\ P_{\text{in}}^{(z)} &= \left\langle \frac{dF_z(t)}{dt} [\rho_a(t) - \rho_d(t)] \right\rangle H. \end{aligned} \quad (5)$$

There are other energy characteristics of the processes considered which might be of physical interest, e.g., the heat outflow from track q and heat flow along axis x , which can be determined using the main characteristics (5).

Equations (1)–(5) provide a starting point for calculating the motor characteristics for a wide range of problem parameters. However, Eq. (1) indicates the coupling between x and z motions, which generally makes the problem hard. Fortunately, the problem can be tackled analytically in a few limiting cases where the coupling can be neglected. In what follows, we consider two such limits: the case of weak longitudinal forcing corresponding to the linear response limit (see Sec. III) and the case of high barriers of the periodic potential with slow forcing where a kinetic description is adequate for the motion not only in the z but also in the x direction (see Sec. IV). The analysis of the two limiting cases reveals the main properties of the motor.

III. LINEAR RESPONSE REGIME

In this section, we focus on the limit of weak forcing $\beta F_x L \ll 1$, where the linear response theory is valid. This regime admits analytical treatment because Eq. (3) for the state population probability $\rho_q(t)$ can be written in a closed form. To make this evident, first consider the Brownian particle motion in the tilted periodic potential $V_q(x; F_x)$, $q = a, d$, under the action of a static tilting force F_x . In this case, the stationary analytical solution for the probability density and the current in state q populated with probability ρ_q is well known [38–40]:

$$\begin{aligned} p_q(x) &= Q^{-1} \rho_q e^{-\beta V_q(x; F_x)} \left[\int_0^L dx e^{\beta V_q(x; F_x)} \right. \\ &\quad \left. - (1 - e^{-\beta F_x L}) \int_0^x dx' e^{\beta V_q(x'; F_x)} \right], \\ J_q &= D Q^{-1} (1 - e^{-\beta F_x L}) \rho_q, \end{aligned}$$

$$\begin{aligned} Q &= \int_0^L dx e^{\beta V_q(x; F_x)} \int_0^L dx e^{-\beta V_q(x; F_x)} \\ &\quad - (1 - e^{-\beta F_x L}) \int_0^L dx e^{-\beta V_q(x; F_x)} \int_0^x dx' e^{\beta V_q(x'; F_x)}. \end{aligned} \quad (6)$$

In the linear response regime, these expressions take the form

$$\begin{aligned} p_q(x) &\approx \left[\int_0^L dx e^{-\beta V_q(x)} \right]^{-1} \rho_q e^{-\beta V_q(x)}, \\ J_q &\approx L^{-1} \zeta_q^{-1} F_x \rho_q, \end{aligned} \quad (7)$$

where ζ_q^{-1} is the effective mobility of the Brownian particle in the periodic potential $V_q(x)$ [41]:

$$\zeta_q^{-1} = \frac{L^2}{\int_0^L dx e^{\beta V_q(x)} \int_0^L dx e^{-\beta V_q(x)}} \zeta^{-1}. \quad (8)$$

Note that $\zeta_d = \zeta$ and the approximate equalities (7) become exact at $q = d$.

With approximate expressions (7) and the transition rates defined in Eq. (1), the net transition current density between the states $r(x)$ appears as

$$r(x) \approx \gamma \left[\int_0^L dx e^{-\beta V_a(x)} \right]^{-1} \rho_a e^{-\beta F_z z_a} - \gamma L^{-1} \rho_d e^{-\beta F_z z_d}. \quad (9)$$

Thus in the linear response limit, $r(x)$ is independent of x becoming zero at the following equilibrium values of $\rho_q^{(0)}$:

$$\rho_a^{(0)} = [1 + W_a \exp f_z]^{-1}, \quad \rho_d^{(0)} = 1 - \rho_a^{(0)}, \quad (10)$$

where

$$W_a^{-1} \equiv L^{-1} \int_0^L dx e^{-\beta V_a(x)}, \quad f_z = F_z H / k_B T. \quad (11)$$

We are now in a position to discuss the case of the time-dependent force $\mathbf{F}(t)$. Suppose that the time modulation is slow, $\tau^{-1} \ll \gamma_0$, which enables the kinetic description of the z -directed motion. Under such a condition, the interstate transition dynamics is independent of the motion in the x direction. This, together with Eq. (7), allows one to write Eq. (3) in the closed form

$$d\rho_a(t)/dt = -[\tilde{\gamma}_{ad}(t) + \tilde{\gamma}_{da}(t)]\rho_a(t) + \tilde{\gamma}_{da}(t), \quad (12)$$

with the renormalized rate constants

$$\begin{aligned} \tilde{\gamma}_{ad}(t) &= \gamma W_a \exp[f_z(t)/2], \\ \tilde{\gamma}_{da}(t) &= \gamma \exp[-f_z(t)/2]. \end{aligned} \quad (13)$$

The periodic solution of Eq. (12) can be obtained from the general solution [42] using the periodic condition $\rho_a(t) = \rho_a(t + \tau)$:

$$\begin{aligned} \rho_a(t) &= s(t) \{ [s^{-1}(\tau) - 1]^{-1} \varphi(\tau) + \varphi(t) \}, \\ \varphi(t) &= \int_0^t \tilde{\gamma}_{da}(t') s^{-1}(t') dt', \\ s(t) &= \exp \left\{ - \int_0^t [\tilde{\gamma}_{ad}(t') + \tilde{\gamma}_{da}(t')] dt' \right\}. \end{aligned} \quad (14)$$

Explicit expressions (7) for the probability currents in the attached and detached states are x independent. Thus in the

linear response regime, Eq. (4) for the average velocity of the directed motion driven by the longitudinal force $F_x(t) - F_l$ with $\langle F_x(t) \rangle = 0$ takes the form

$$\mathcal{U} = -[\zeta_a^{-1} \langle \rho_a(t) \rangle + \zeta^{-1} (1 - \langle \rho_a(t) \rangle)] F_l + (\zeta_a^{-1} - \zeta^{-1}) \langle \rho_a(t) F_x(t) \rangle. \quad (15)$$

A. Adiabatic limit

In the adiabatic limit $\tau^{-1} \ll \gamma$, the population probability can be taken as $\rho_a(t) = [1 + W_a \exp f_z(t)]^{-1}$ [cf. Eq. (10)], so that the main motor characteristics defined in Eqs. (4) and (5) can be easily found for the symmetric rectangular excitation of the form $\mathbf{F}(t) = \mathbf{F} \text{sign}[\sin(2\pi t/\tau)]$ [where $\text{sign}(\xi) = 1$ at $\xi > 0$ and $\text{sign}(\xi) = -1$ at $\xi < 0$] from the relations

$$\begin{aligned} \mathcal{U} &= \Phi_0 (\Phi_1 F_x - F_l), \quad P_{\text{in}}^{(x)} = \Phi_0 F_x^2, \\ P_{\text{in}}^{(z)} &= \frac{8k_B T}{\tau} \frac{W_a \sinh f_z}{1 + W_a^2 + 2W_a \cosh f_z} f_z, \\ \Phi_0 &= \frac{\zeta^{-1} W_a (W_a + \cosh f_z) + \zeta_a^{-1} (1 + W_a \cosh f_z)}{1 + W_a^2 + 2W_a \cosh f_z}, \\ \Phi_1 &= \frac{(\zeta^{-1} - \zeta_a^{-1}) W_a \sinh f_z}{\zeta^{-1} W_a (W_a + \cosh f_z) + \zeta_a^{-1} (1 + W_a \cosh f_z)}. \end{aligned} \quad (16)$$

In the unloaded regime $F_l = 0$, the expression for the average velocity is greatly simplified:

$$\mathcal{U} = \zeta_{\text{eff}}^{-1} F_x, \quad \zeta_{\text{eff}}^{-1} \equiv \frac{(\zeta^{-1} - \zeta_a^{-1}) W_a \sinh f_z}{1 + W_a^2 + 2W_a \cosh f_z}. \quad (17)$$

As an example, for the sawtooth potential $V_a(x)$ of the amplitude U with the average value U_0 [relative to the energy of the detached state $V_d(x) = 0$, see Fig. 1] and for the case of the zero value of the temporal asymmetry parameter $\varepsilon = 0$ (see Fig. 2), the quantities W_a and ζ_a^{-1} are given by the relations

$$W_a = \frac{u}{\sinh(u)} \exp(u_0), \quad \zeta_a^{-1} = \frac{u^2}{\sinh^2(u)} \zeta^{-1}, \quad (18)$$

where $u \equiv \beta U$ and $u_0 \equiv \beta U_0$. First of all, note that expressions (18) do not depend on the asymmetry of the potential $V_a(x)$ (characterized by the parameter l). So the directional motion occurs, in particular, for a symmetric potential. The effective mobility of the Brownian particle in the attached state ζ_a^{-1} is determined only by the amplitude of potential $V_a(x)$, whereas the quantity W_a depends on both U and U_0 . Thus, in the low-temperature limit ($u, u_0, f_z \rightarrow \infty$), where $\zeta_a^{-1} \approx 4u^2 \exp(-2u) \zeta^{-1}$, $W_a \approx 2u \exp(u_0 - u)$, and $W_a \cosh f_z \approx u \exp(u_0 - u + f_z)$, the effective mobility ζ_{eff}^{-1} tends to zero at $F_z H < |U - U_0|$ and takes the maximum value $\zeta^{-1}/2$ at $F_z H > |U - U_0|$. At the same time, the effective mobility ζ_{eff}^{-1} vanishes in both cases for high temperatures, since $\zeta_a^{-1} \rightarrow \zeta^{-1}$ at $u \rightarrow 0$. That is why the temperature dependence of the velocity is nonmonotonic at $F_z H < |U - U_0|$ and monotonic at $F_z H \geq |U - U_0|$. Such behavior is depicted in Fig. 3 for the case $U_0 = 0$.

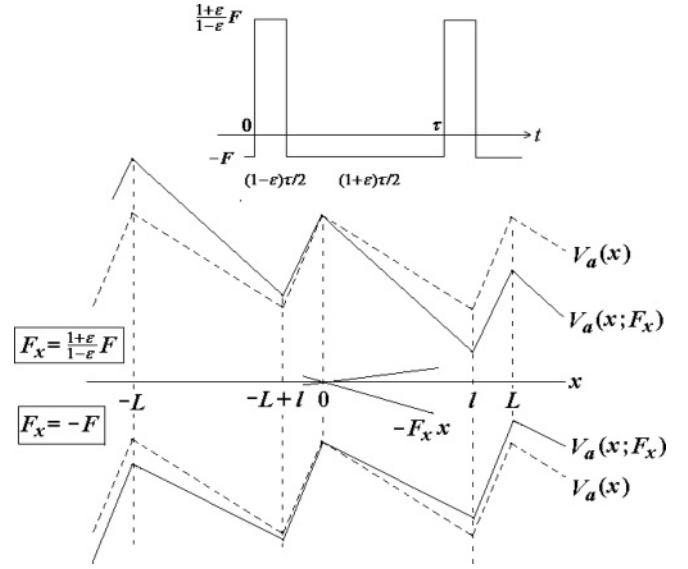


FIG. 2. Dichotomic fluctuations of the applied unbiased force and the fluctuation-induced change in the sawtooth potential $V_a(x)$.

The compact expression for the efficiency can be derived from Eqs. (5) and (16) by neglecting the quantity $P_{\text{in}}^{(z)}$, which is justified in the adiabatic limit

$$\eta = \frac{F_l (\Phi_1 F_x - F_l)}{F_x^2}. \quad (19)$$

From Eq. (19) it follows that the maximum of the efficiency as the function of F_l is $\eta_{\text{max}} = \Phi_1^2/4$. The temperature dependence of η_{max} is presented in the framed inset in Fig. 3. If $\zeta_a \gg \zeta$, then Eq. (16) for Φ_1 can be used to estimate the upper bound of η_{max} :

$$\eta_{\text{max}} = \frac{1}{4} \frac{\sinh^2 f_z}{(W_a + \cosh f_z)^2} < \frac{1}{4}. \quad (20)$$

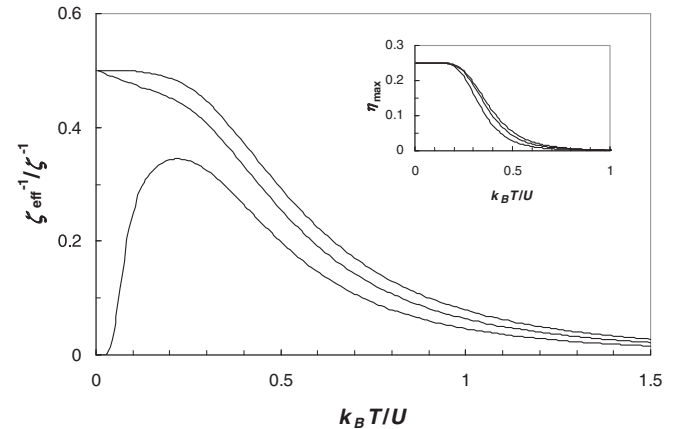


FIG. 3. The temperature dependences of the effective mobility defined by Eq. (17) for the sawtooth potential $V_a(x)$. The curves in descending order correspond to the respective ratios $F_z H/U$ of 1.3, 1, and 0.7 at $U_0 = 0$. The top right frame shows the temperature dependences of the maximum efficiency for the same values of $F_z H/U$.

B. Beyond the adiabatic limit

To go beyond the adiabatic limit, we invoke the additional approximation that transverse forcing is also weak, $|f_z(t)| \ll 1$. Then the expansion of solution (14) in terms of the small periodic functions $f_z(t)$ yields

$$\begin{aligned} \rho_a(t) = & \frac{1}{1+W_a} \left\{ 1 - \frac{\gamma W_a}{\exp[\gamma(1+W_a)\tau] - 1} \int_0^\tau dt' f_z(t') \right. \\ & \times \exp \left[-\gamma(1+W_a)(t-t') - \gamma W_a \int_0^{t'} dt' f_z(t') \right] \\ & \left. \times \exp[-\gamma(1+W_a)(t-t')] \right\}. \end{aligned} \quad (21)$$

The expression obtained indicates that there is a delay of the population probability $\rho_a(t)$ with respect to the transverse forcing $f_z(t)$. The characteristic time of this delay is $[\gamma(1+W_a)]^{-1}$. Such a delay occurs for sufficiently high barriers V_z between the attached and detached states and for not too large values of the parameter W_a when the inequality $\gamma(1+W_a) \ll \gamma_0 \sim k_B T / \zeta H^2$ holds. On the other hand, it is known [18] that the adiabatic approximation $J_a[F_x(t), t] \approx J_a[F_x(t)]$ is valid if the excitation frequency satisfies the condition $\tau^{-1} \ll k_B T / \zeta L^2$. Thus, with τ^{-1} falling in the above range and $H \sim L$, one can take advantage of the adiabatic approximation and use Eq. (21). At the same time, τ can be larger or smaller than the delay time $[\gamma(1+W_a)]^{-1}$.

The desired characteristics of the motor are derived by the substitution of Eq. (21) into Eqs. (5) and (15). The average velocity \mathfrak{U} is most simply represented in terms of the Fourier components f_j of the applied forces $f(x)$ [$f(x) = \sum_j f_j \exp(-i\omega_j t)$, $\omega_j = 2\pi j/\tau$, where j is an integer]:

$$\begin{aligned} \mathfrak{U} = & -\frac{W_a \zeta^{-1} + \zeta_a^{-1}}{1+W_a} F_l \\ & + \gamma \frac{(\zeta^{-1} - \zeta_a^{-1}) W_a}{1+W_a} \sum_j \frac{F_{x,j} f_{z,-j}}{\gamma(1+W_a) + i\omega_j}. \end{aligned} \quad (22)$$

In the particularly important case of two mixed sinusoidal signals, $F_x(t) = F_x \cos \omega t$ and $F_z(t) = F_z \cos(\omega t - \varphi)$, mutually phase shifted by φ , Eq. (22) leads to

$$\begin{aligned} \mathfrak{U} = & -\frac{W_a \zeta^{-1} + \zeta_a^{-1}}{1+W_a} F_l + \frac{(\zeta^{-1} - \zeta_a^{-1}) W_a}{2(1+W_a)^2} S(\tilde{\omega}) F_x f_z, \\ S(\tilde{\omega}) = & \frac{\cos \varphi + \tilde{\omega} \sin \varphi}{1 + \tilde{\omega}^2}, \quad \tilde{\omega} \equiv \frac{\omega}{\gamma(1+W_a)}. \end{aligned} \quad (23)$$

Here the function $S(\tilde{\omega})$ accounts for the delayed response of the system to the external excitation (see Fig. 4). It decreases from unity (in the adiabatic limit) to zero at $\varphi = 0$ and exhibits a nonmonotonic behavior at $\varphi \neq 0$, with a stopping point emerging at $\varphi < 0$. The maximum value of the efficiency is reached in the adiabatic limit at $\varphi = 0$. It is defined as follows:

$$\eta_{\max} = \frac{1}{8} \frac{f_z^2}{(W_a + 1)^2}. \quad (24)$$

The efficiency is small due to the smallness of the parameter f_z .

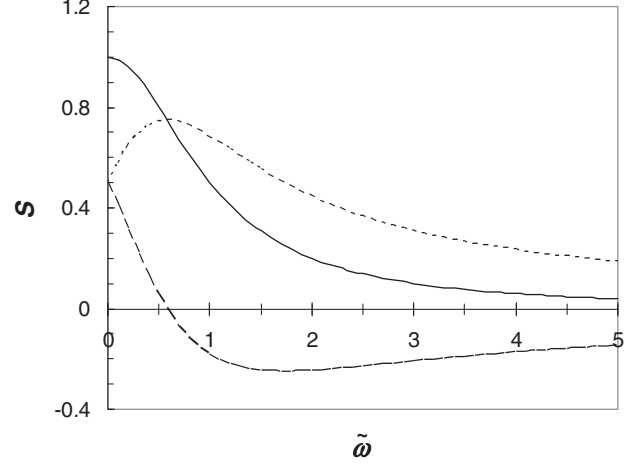


FIG. 4. The quantity $S(\tilde{\omega})$ versus the modulation frequency (scaled by the reciprocal delay time) for different values of the phase shift between the two force components: $\varphi = 0$ (the solid line), $\varphi = \pi/3$ (the long-dashed line), and $\varphi = -\pi/3$ (the short-dashed line). Note that the average velocity \mathfrak{U} is proportional to $S(\tilde{\omega})$.

IV. KINETIC DESCRIPTION

In this section, we consider another physical situation amenable to analytical treatment. Assume that a Brownian particle moves in a periodic potential with interwell barrier heights larger than the particle thermal energy $k_B T$ and the potential modulation frequency much less than the inverse time D/L^2 of the particle diffusion over the spatial period L . Then the particle motion in the x direction can be regarded as thermally activated hopping between the potential wells (discrete states). With this coarse-grained description, one can neglect the details of the particle intrawell behavior, in particular, the coupling to the transverse dynamics [see Eq. (1)]. Thus the motions in the x and z directions can be described separately. A further advantage of the kinetic approach is that it allows going beyond the linear response regime, thus providing a possibility to elucidate the role of inherent and induced asymmetry in the emergence of directed motion.

Within the kinetic description, the probability current is simply the difference between the hopping rates to the right and to the left. The corresponding forward and reverse rate constants $\vec{\alpha}$ and $\bar{\alpha}$ can be found [43,44] by calculating the probabilities to overcome the barrier at $x = 0$ from the left to the right and vice versa (see Fig. 2):

$$\begin{aligned} \vec{\alpha} = & \frac{D}{\int_{-L+1}^L dx e^{\beta V_a(x; F_x)} \int_{-L}^0 dx e^{-\beta V_a(x; F_x)}}, \\ \bar{\alpha} = & \frac{D}{\int_{-L+1}^L dx e^{\beta V_a(x; F_x)} \int_0^L dx e^{-\beta V_a(x; F_x)}}. \end{aligned} \quad (25)$$

Using the equality $\int_{-L}^0 dx e^{-\beta V_a(x; F_x)} = e^{-\beta F_x L} \int_0^L dx e^{-\beta V_a(x; F_x)}$ which follows from definition (1) of $V_q(x; F_x)$, we obtain the probability current in the attached state under

the action of the homogeneous and stationary force F_x :

$$J_a = (\bar{\alpha} - \tilde{\alpha})\rho_a^{(0)} = \frac{D(e^{\beta F_x L} - 1)}{\int_{-L+1}^1 dx e^{\beta V_a(x; F_x)} \int_0^L dx e^{-\beta V_a(x; F_x)}} \rho_a^{(0)}, \quad (26)$$

where the state population probability $\rho_a^{(0)}$ is defined by Eq. (10). The current in the detached state is $J_d = L^{-1}\zeta^{-1}F_x\rho_d^{(0)}$. Thus for the asymmetric sawtooth potential $V_a(x)$ of the amplitude U , with $U_0 = 0$ (see Figs. 1 and 2), the total probability current reads

$$J(\mathbf{F}) = \frac{U}{\zeta L^2} \frac{4}{1 + 2ue^{-u+f_z}} \times \{ue^{-2u}[e^{f_x(1-\kappa)} - e^{f_x(1+\kappa)}] + f_x e^{-u+f_z}\}, \quad (27)$$

with the asymmetry coefficient $\kappa = (2l - L)/L$ and the dimensionless parameters $u = \beta U > 1$ and $f_x = \beta F_x L/2 < u$. Note that beyond the linear response, $f_x \gtrsim 1$, spatial asymmetry comes into play.

To rationalize the role of inherent and induced asymmetry in controlling particle transport, consider a simple case of a time-periodic rectangular asymmetric excitation $\mathbf{F}(t)$. The positive and negative force pulses are different both in magnitude and duration but the period-averaged force vanishes, $\langle \mathbf{F}(t) \rangle = 0$ (see Fig. 2). The excitation gives rise to the directed motion of the particle, with the velocity \mathcal{U} which, in the adiabatic limit and at the zero load force, becomes

$$\mathcal{U} = \frac{L}{2} \left[(1 - \varepsilon) J \left(\frac{1 + \varepsilon}{1 - \varepsilon} \mathbf{F} \right) + (1 + \varepsilon) J(-\mathbf{F}) \right]. \quad (28)$$

[Here ε is the temporal asymmetry parameter defined in Fig. 2 such that $|\varepsilon| < 1$ and $J(\mathbf{F})$ is specified by Eq. (27).]

Figure 5 illustrates the peculiarities of the velocity change with temperature in different regimes. As panel (a) indicates, (i) there is no current reversal upon varying the temperature in the absence of spatial and temporal asymmetry (curve 1); (ii) spatial asymmetry leads to the appearance of current reversal (curve 2); and (iii) in the case $f_z = 0$ when our model reduces to the rocking ratchet scheme, a stopping point can arise as a result of the competition between spatial (inherent) and temporal (induced) asymmetry (curve 3). The curves in Figs. 5(b) and 5(c) show the possibility for one or two stopping points to arise, with the different scale of the velocity magnitude. Thus the ratio $F_z H/U$ and the asymmetry parameters κ and ε , along with the additionally introduced phase shift between force components and the load force, may have a dramatic impact on the temperature behavior of the velocity causing, in particular, multiple current reversals.

Estimating the characteristic values of the average velocity, we use the typical sliding velocity $U/(\zeta L)$ as a scaling factor (see Fig. 5). For characteristic parameter values $U = 10$ pN nm, $\zeta = 10^{-6}$ pN s/nm, and $L = 10$ nm, the sliding velocity is sufficiently high, $U/(\zeta L) = 10^3 \mu\text{m/s}$. As a result, the velocity of the motor treated here can amount to biologically relevant values of the order $100 \mu\text{m/s}$ [see Fig. 5(a)].

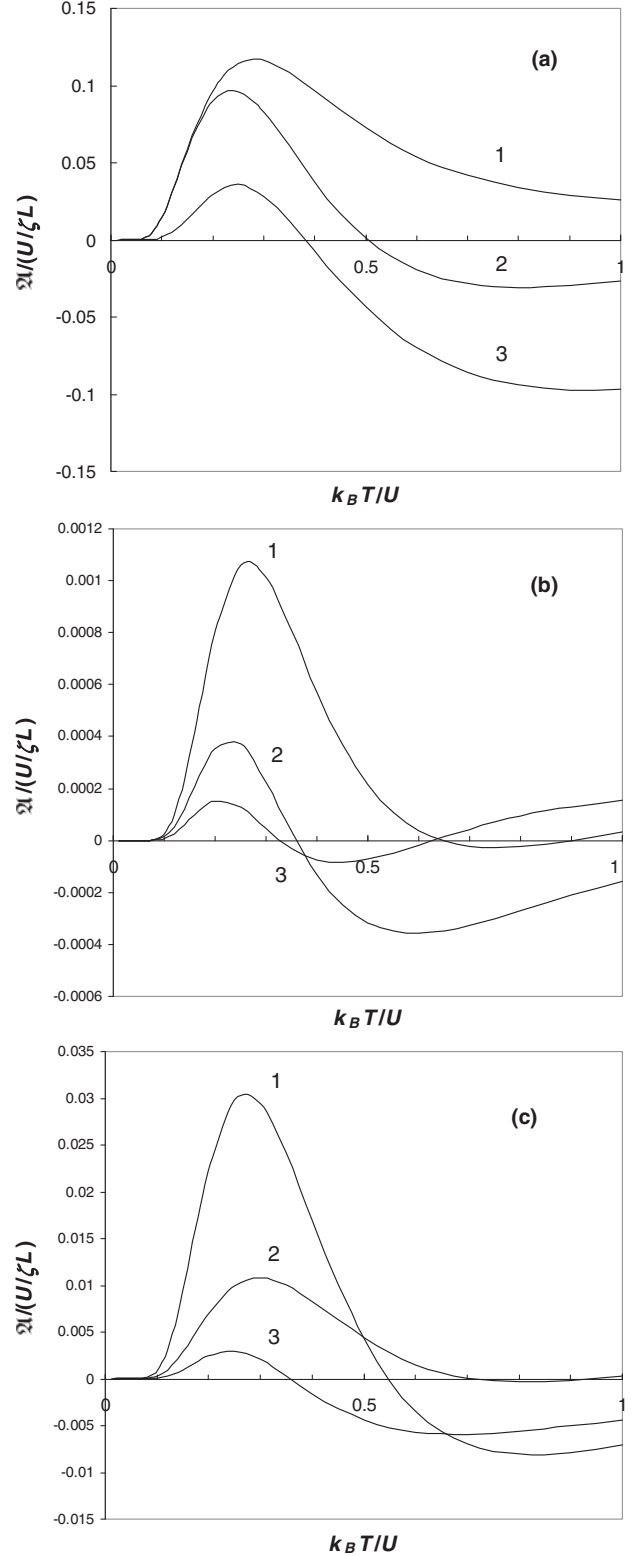


FIG. 5. The temperature dependences of the average velocity in the framework of the kinetic approach with $f_x/u = 0.3$ and the system parameters $f_z/u \equiv \delta$, κ , and ε varied: curves 1, 2, and 3, respectively, correspond to (a) $\delta = 0.3$, $\kappa = \varepsilon = 0$; $\delta = 0.3$, $\kappa = 0.9$, $\varepsilon = 0$; and $\delta = 0$, $\kappa = 0.8$, $\varepsilon = 0.55$; (b) $\delta = 0.04$, $\kappa = 0$, $\varepsilon = -0.75$; $\delta = 0.02$, $\kappa = 0$, $\varepsilon = -0.75$; and $\delta = 0.01$, $\kappa = -0.05$, $\varepsilon = -0.75$; and (c) $\delta = 0.3$, $\kappa = 0.5$, $\varepsilon = -0.3$; $\delta = 1.5$, $\kappa = 0.8$, $\varepsilon = -0.8$; and $\delta = 0.3$, $\kappa = 0.8$, $\varepsilon = -0.8$.

V. DISCUSSION AND CONCLUSIONS

The model developed in the present study exhibits a rich variety of behaviors, some of which are sufficiently simple to be tractable analytically. In the trivial cases, where only one of two above-discussed fluctuating forces is applied, our model reproduces one of two paradigmatic scenarios for noise-induced motion, flashing and rocking (or asymmetrically tilting) ratchets. Indeed, if only the transverse excitation F_z is fed, directed motion arises due to potential profile fluctuations so that the flashing ratchet scheme is implemented. In this case, spatial asymmetry and nonadiabatic conditions are crucial for the effect to emerge (in symmetric systems, accelerated diffusion is only possible [45]). We do not intend to discuss these features in further detail here, as the flashing ratchet has been abundantly discussed in the literature.

With only the longitudinal excitation F_x , our model operates as a rocking (or asymmetrically tilting) ratchet. Importantly, this motor efficiently functions in the adiabatic limit provided that the potential profile is asymmetric. When both F_x and F_z are applied, the suggested model is not merely a hybrid of the two prototypical mechanisms, but exhibits qualitatively new features as compared to either of them. In particular, if the force components fluctuate synchronously, neither the spatial asymmetry of the potential nor the temporal asymmetry of input signals is necessary for directed motion to occur. This case exemplifies the gating mechanism [12,32,33] thoroughly analyzed in the low-energy approximation [22].

The Brownian motor considered here has some features in common with the so-called near-surface motor [35] in which the unidirectional surface-parallel motion of a Brownian particle is produced by a surface-inclined zero-mean small fluctuating force. This motor operates in the near-surface potential $V(x,z)$ which is periodic in the surface-parallel coordinate x and, in the case of a polar substrate, exponentially fast decreases with distance z , with the zero average value of $V(x,z)$. This peculiarity corresponds to $U_0 = 0$ in the present model. A key distinction between these two models is that the transverse motion involved in the present model is restricted by transitions between the attached and detached states which are delayed relative to the fluctuations of the transition-inducing transverse force component. Though somewhat simplistic, this description of transverse motion captures the essentials of the problem and, importantly, makes the analytical treatment quite feasible. On the other hand, this setup is relevant to a variety of situations where the moving part of a motor can be attached to or detached from the track-parallel surface depending on its conformational state. If this motor part carries a charge, it can be driven by an ac electric signal.

A distinctive feature of the present analysis is that it includes a delayed system response to external force signals. This is possible since the attached/detached state lifetime and the characteristic time of diffusion over the potential period differ widely, $L^2/D \ll \gamma^{-1}$, which allows us to simultaneously consider the delayed response of the state populations and the adiabatic limit for the longitudinal motion. For the particularly important case of two mixed sinusoidal signals, $F_x(t) =$

$F_x \cos \omega t$ and $F_z(t) = F_z \cos(\omega t - \varphi)$, with the frequency $\omega \ll D/L^2$, it is then found (see Sec. III and Fig. 4) that the motor velocity \mathfrak{U} (i) monotonically decreases with ω if the synchronous signals are coherent, $\varphi = 0$ (solid line), and (ii) behaves nonmonotonically as a function of ω if there is a phase shift between the signals, $\varphi \neq 0$ (short-dashed line). The long-dashed line in Fig. 4 demonstrates that certain values of the phase shift can result in a stopping point on different sides of which the function $\mathfrak{U}(\omega)$ has the opposite signs.

The most striking manifestation of the effect is that directed motion emerges even in the absence of spatial and temporal asymmetry provided the input force signals are synchronized. In this situation, Eqs. (16) and (17) suggest that the model exhibits qualitatively different behaviors, depending on the signal amplitudes. In particular, the low-temperature trends in the probability current are different at $F_z H < |U - U_0|$ and $F_z H \geq |U - U_0|$: in the former case, the current tends to zero as $T \rightarrow 0$, while in the latter, it takes the maximum value in this limit. Hence, the respective temperature dependences of the velocity are nonmonotonic and monotonically decreasing (see Fig. 3 for the case of $U_0 = 0$). The maximum efficiency can reach 0.25 in the low-temperature limit.

The spatial asymmetry of the potential and the temporal asymmetry of the excitations are the governing factors of the current reversal occurrence. Their effect on motion characteristics is analyzed in terms of the kinetic approach which enables simplification of the analysis as well as extension of the resulting conclusions to arbitrarily shaped potentials. As shown in Sec. IV (see Fig. 5), both spatial and temporal asymmetry afford the possibility of current reversal. Two stopping points originate from the competition between the two kinds of asymmetry. It is evident that a richer behavior of the motor velocity exhibited, in particular, by multiple current reversals, may follow from a more sophisticated treatment which additionally includes such factors as a delayed response of state populations, a phase shift between the F_x and F_z force components (as in Sec. III), and the load force F_l .

Substituting the biologically relevant values of model parameters into the analytical relationships obtained, one can estimate the characteristic average velocities of the suggested motor which in some regimes are comparable to those of typical (protein) molecular motors (100 nm/s). A simple mechanism of directed motion generation along with a high estimated efficiency of the corresponding Brownian motor offer much promise for research- and practice-oriented implementations of the model developed.

ACKNOWLEDGMENTS

The authors thank M. L. Dekhtyar for helpful comments on this paper. This work was supported by National Chiao Tung University and Academia Sinica. V.M.R. thanks the Complex Program for Basic Research of the National Academy of Sciences of Ukraine for partial support (Grant No. 3/11-H). Yu.A.M. thanks the Russian Foundation for Basic Research for partial support (Grant No. 10-03-00393). Yu.A.M. and V.M.R. gratefully acknowledge the kind hospitality received from the Institute of Atomic and Molecular Sciences.

- [1] F. Jülicher, A. Ajdari, and J. Prost, *Rev. Mod. Phys.* **69**, 1269 (1997).
- [2] R. D. Astumian, *Science* **276**, 917 (1997).
- [3] P. Reimann, *Phys. Rep.* **361**, 57 (2002).
- [4] R. Bartussek and P. Hänggi, *Phys. Bl.* **51**, 506 (1995).
- [5] H. Qian, *Biophys. Chem.* **67**, 263 (1997).
- [6] R. D. Astumian and P. Hänggi, *Phys. Today* **55**(11), 33 (2002).
- [7] P. Reimann and P. Hänggi, *Appl. Phys. A* **75**, 169 (2002).
- [8] J. M. R. Parrondo and B. J. de Cisneros, *Appl. Phys. A* **75**, 179 (2002).
- [9] P. Hänggi, F. Marchesoni, and F. Nori, *Ann. Phys. (Leipzig)* **14**, 51 (2005).
- [10] E. R. Kay, D. A. Leigh, and F. Zerbetto, *Angew. Chem., Int. Ed.* **46**, 72 (2006).
- [11] J. Vacek and J. Michl, *Adv. Funct. Mater.* **17**, 730 (2007).
- [12] P. Hänggi and F. Marchesoni, *Rev. Mod. Phys.* **81**, 387 (2009).
- [13] J. Howard, *Mechanics of Motor Proteins and the Cytoskeleton* (Sinauer Associates, Sunderland, 2001).
- [14] B. Hille, *Ionic Channels of Excitable Membranes* (Sinauer Associates, Sunderland, 1992).
- [15] K. E. Drexler, *Nanosystems: Molecular Machinery, Manufacturing and Computation* (Wiley, New York, 1992).
- [16] A. L. R. Bug and B. J. Berne, *Phys. Rev. Lett.* **59**, 948 (1987).
- [17] A. Ajdari and J. Prost, *C. R. Acad. Sci. Paris Ser. II* **315**, 1635 (1992).
- [18] R. D. Astumian and M. Bier, *Phys. Rev. Lett.* **72**, 1766 (1994).
- [19] M. O. Magnasco, *Phys. Rev. Lett.* **71**, 1477 (1993).
- [20] C. R. Doering, W. Horsthemke, and J. Riordan, *Phys. Rev. Lett.* **72**, 2984 (1984).
- [21] R. Bartussek, P. Hänggi, and J. G. Kissner, *Europhys. Lett.* **28**, 459 (1994).
- [22] V. M. Rozenbaum, *Zh. Eksp. Teor. Fiz.* **137**, 740 (2010) [*JETP* **110**, 653 (2010)].
- [23] V. M. Rozenbaum, T. Ye. Korochkova, A. A. Chernova, and M. L. Dekhtyar, *Phys. Rev. E* **83**, 051120 (2011).
- [24] A. Ajdari, D. Mukamel, L. Peliti, and J. Prost, *J. Phys. I* **4**, 1551 (1994).
- [25] J. Luczka, R. Bartussek, and P. Hänggi, *Europhys. Lett.* **31**, 431 (1995).
- [26] D. R. Chialvo and M. M. Millonas, *Phys. Lett. A* **209**, 26 (1995).
- [27] M. C. Mahato and A. M. Jayannavar, *Phys. Lett. A* **209**, 21 (1995).
- [28] K. Seeger and W. Maurer, *Solid State Commun.* **27**, 603 (1978).
- [29] W. Wonneberger, *Solid State Commun.* **30**, 511 (1979).
- [30] F. Marchesoni, *Phys. Lett. A* **119**, 221 (1986).
- [31] I. Goychuk and P. Hänggi, *Europhys. Lett.* **43**, 503 (1998).
- [32] S. Savel'ev, F. Marchesoni, P. Hänggi, and F. Nori, *Europhys. Lett.* **67**, 179 (2004).
- [33] S. Savel'ev, F. Marchesoni, P. Hänggi, and F. Nori, *Phys. Rev. E* **70**, 066109 (2004).
- [34] J. D. Bao, Y. Abe, and Y. Z. Zhuo, *Physica A* **277**, 127 (2000).
- [35] V. M. Rozenbaum and A. A. Chernova, *Surf. Sci.* **603**, 3297 (2009).
- [36] L. Jullien, A. Lemarchand, and H. Lemarchand, *J. Chem. Phys.* **112**, 8293 (2000).
- [37] D. Alcor, V. Croquette, L. Jullien, and A. Lemarchand, *Proc. Natl. Acad. Sci. USA* **101**, 8276 (2004).
- [38] R. L. Stratonovich, *Radiotekh. Elektron. (Moscow)* **3**, 497 (1958).
- [39] H. Risken, *The Fokker-Planck Equation* (Springer, Berlin, 1984).
- [40] P. Reimann, C. Van den Broek, H. Linke, P. Hänggi, J. M. Rubi, and A. Perez-Madrid, *Phys. Rev. Lett.* **87**, 010602 (2001).
- [41] S. Lifson and J. L. Jackson, *J. Chem. Phys.* **36**, 2410 (1962).
- [42] L. Gammaitoni, P. Hänggi, P. Jung, and F. Marchesoni, *Rev. Mod. Phys.* **70**, 223 (1998).
- [43] V. M. Rozenbaum, D.-Y. Yang, S. H. Lin, and T. Y. Tsong, *Physica A* **363**, 211 (2006).
- [44] V. M. Rozenbaum, Yu. A. Makhnovskii, D.-Y. Yang, S.-Y. Sheu, and S. H. Lin, *J. Phys. Chem. B* **114**, 1959 (2010).
- [45] A. A. Dubkov and B. Spagnolo, *Phys. Rev. E* **72**, 041104 (2005).